SHEAR BEHAVIOUR OF STEEL FIBRE REINFORCED SELF-CONSOLIDADTING CONCRETE BEAMS BASED ON THE MODIFIED COMPRESSION FIELD THEORY

Yining DING [1), Fasheng ZHANG [1), Torgal Fernando [2) and Yulin ZHANG [3)

[1) State Key Laboratory of Coastal and Offshore Engineering
Dalian University of Technology
116024 Dalian, China
[2) Research Unit C-TAC (Sustainable Construction Branch)

4800-058 Guimarães, Portugal

[3) Centre of Mathematics, University of Minho

4700-052, Portugal

Key words: Steel fibres, Self-consolidating concrete beam, Modified compression field theory, Shear capacity, Hybrid effect.

Abstract: A series of steel fibre reinforced self-consolidating concrete (SFRSCC) beams have been tested to investigate the influence of steel fibres and the combined effect of fibers and stirrups on the deflection and cracking, ultimate loads and failure pattern. The experiment indicates that the shear strength increases clearly with the increasing of fibre content. The combination of steel fibres and stirrups demonstrates a positive composite effect on the ultimate load, ductility and failure pattern of concrete beam. This study also examines the feasibility of applying the modified compression field theory (MCFT) for the suitable assessment of shear resistance in fibre and steel rebar reinforced self-consolidating concrete beams. For fibre reinforced concrete member, a theoretical method is proposed based on the MCFT. The proposed ultimate shear capacity model was verified by the comparison with different test results.

1 INTRODUCTION

Concrete has low tensile strength and fails in a brittle manner. If fibres are added to the classical components of concrete, the steel fibre reinforced concrete (SFRC) can show higher toughness under static loading, such as tension, bending and shear. Steel fibres in the concrete can also enhance the mechanical properties, ductility and energy absorbing capacity under seismic, impact and blast loading [1]. One of the most important functions of steel fibres in concrete is the ability to transfer stresses across the cracked section, providing to concrete a residual strength, which magnitude depends on the fibre, matrix and fibre-matrix properties. The application of fibre reinforced self-consolidating concrete (SFRSCC) is one of the major part of special SCC. To increase the efficiency of steel fibres in concrete matrix, SFRSCC combines the benefits of SCC in the fresh state and shows some improved performances in the hardened state of steel fibre reinforced concrete (SFRC), especially the bond property between the fibre and the concrete matrix [2]. The most efficient applications of SFRSCC are those where the fibres can replace the conventional reinforcement. Some examples are

applications in industrial floors, support of tunnellings, beams [3-6]. Nonetheless, the structural use of SFRSCC in the concrete industry has not yet been fully achieved because a design procedure that considers the randomly distributed discrete fibre behaviour across cracks in a rational manner is very rare.

Previous studies of shear carried out for structural applications of fibre reinforced concrete include slender and deep beams, with or without transverse reinforcement [7-15]. These studies indicate that the addition of fibres can greatly improve the shear capacity of beams. Fibres can be used either to boost the shear capacity or to replace, in part, the vertical stirrups in conventional reinforced concrete structural members. Although numerous experimental and theoretical investigations on shear problems of various fibrous concrete beams have been made during the past three decades, few are concerned with SFRSCC beams. Test data available on the reinforcing effect of fibres in the self-consolidating concrete members failing in shear are rather limited [16-17]. Most design code methods in treating shear still rely on empirical formulas, although some recent approaches, such as the plasticity theory or the modified compression field theory (MCFT), can be regarded as rational in the sense that they are capable of providing physical significance [13, 18-19].

This study examines the feasibility of applying the MCFT for the rational assessment of shear resistance in steel fibre-reinforced self-consolidating concrete beams, while providing experimental data to support the theory proposed, as well as to extend the current experimental database. An experimental program was therefore conducted to study the shear behaviour of SFRSCC beams containing longitudinal bars and vertical stirrups. Moreover, the hybrid effect of steel fibres and stirrups on the mechanical behaviour of beams was also studied.

2 PROPOSED METHODS BASED ON MCFT

The MCFT [20] is a further development of the CFT (compression field theory) that accounts for the influence of the tensile stresses in the cracked concrete. It was developed by observing the response of a large number of reinforced concrete (RC) elements loaded in pure shear or shear combined with axial stress. The relationship of the MCFT can be used to predict the shear strength of a beam subjected to shear, moment and axial load. The simplified MCFT for calculating shear strength of RC elements was also proposed [21-22]. In these models, the cracked concrete is treated as a new material with its own stress-strain characteristics. It is interesting to note that the fibre reinforced concrete is more suitable than plain concrete for the application of MCFT, due to its flatter stress-strain relationship in the post-peak range in compression and in tension than that of plain concrete, the studies of shear problems reflecting this are absent. The contribution of fibres to the shear capacity of SFRC can be taken into account based on the MCFT.

Failure of the RC element may be governed not by average stresses, but rather by local stresses that occur at a crack [20, 23]. In checking the conditions at a crack, the actual complex crack pattern is idealized as a series of parallel cracks, all occurring at angle θ to the longitudinal reinforcement and space a distance S_θ apart. For a free-body diagram of part of fibre reinforced concrete element, Fig.1 compares the calculated average stresses (Plane 1 in

Fig. 1a) with the actual local stresses that occur at a crack (Plane 2 in Fig.1b). The critical crack direction is assumed normal to the principal tensile strain direction. While the calculated average shear stress on Plane 1 is zero, there may be local shear stresses on Plane 2.

As the applied external stresses are fixed, the two sets of stresses shown in Fig.1a and Fig.1b must be statically equivalent. Assuming a unit area for both Plane 1 and Plane 2, the requirement that the two sets of stresses produce the same force in the z-direction is
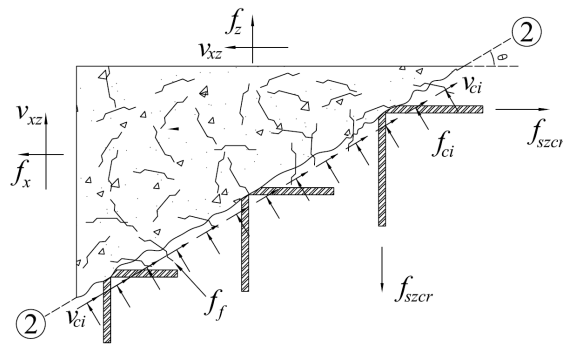
$$\rho_{sz}f_{sz}cos\theta + f_{1}cos\theta = \rho_{sz}f_{szcr}cos\theta - f_{ci}\,cos\theta + v_{ci}sin\theta + v_{f}\,sin\theta + \sigma_{f}\,cos\theta \qquad (1)$$

At high loads, the average strain in the stirrups ε_z will typically exceed the yield strain of transverse steel. In this situation, both f_{sz} and f_{szcr} will equal the yield stress in the stirrups, and then we can get Eqn. (2):
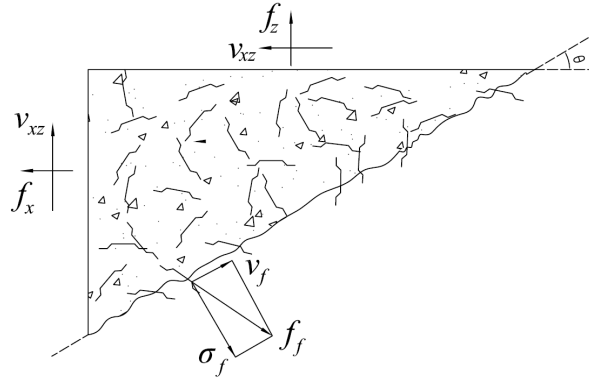
$$f_1 = (v_{ci} + v_f)\,tan\theta + \sigma_f \qquad (2)$$
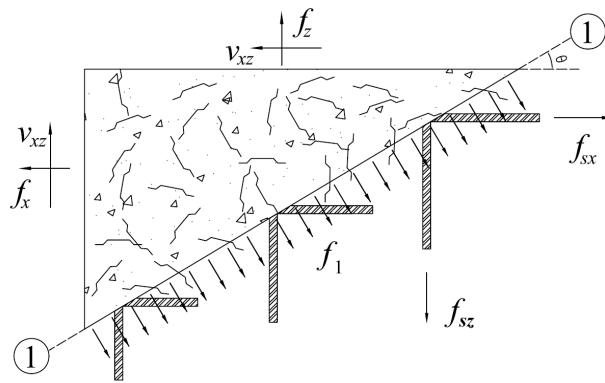
(a) Calculated Average Stresses

(b) Local Stresses at a Crack

3

(c) Stress component of a single fibre transferred perpendicular to crack and parallel to crack

Fig.1 Comparison of local stresses at a crack with calculated average stresses of SFRC and stress state of a single fibre

A simplified concept for anisotropic contributions by hooked or paddled fibres to post-peak strength has been suggested by Stroeven P. in Eqn. (3) as follows [24-25]

$$\sigma_f = \nu_f = \alpha \tau_f V_f (1+f)(1+\omega_2 / 2)(1-4w / l_f) / 3 \qquad (3)$$

Where

α = the aspect ratio ($\alpha = l_f / d_f$. l_f, d_f are the length and diameter of fibres, respectively);

τ_f = the average fibre matrix interfacial bond stress;

V_f = the volume fraction of fibres;

ω_2 = the degree of planar orientation;

w = the average crack width;

f = the coefficient of friction between concrete and fibre sheared over the crack edge;

In the MCFT [20], equilibrium, compatibility and constitutive relationships are formulated in terms of average stresses and average strains. Relevant equations used in the MCFT for SFRC are summarized in Table 1.

Table 1 Equations of modified compression field theory for fibre reinforced concrete

| | Geometric conditions: | Stress-strain relationships: |

Equilibrium:	Average strains:	Reinforcement:
Average stresses: $$f_x = \rho_x f_{sx} + f_1 - v\cot\theta \quad (4)$$ $$f_z = \rho_z f_{sz} + f_1 - v\tan\theta \quad (5)$$ $$v = (f_1 + f_2)/(\tan\theta + \cot\theta) \quad (6)$$ Stresses at cracks: $$f_{sxcr} = (f_x + v\cot\theta + v_a\cot\theta)/\rho_x \,(7)$$ $$f_{szcr} = (f_z + v\tan\theta - v_{ci}\tan\theta)/\rho_z \,(8)$$	$$\tan^2\theta = \frac{\varepsilon_x + \varepsilon_2}{\varepsilon_z + \varepsilon_2} \quad (9)$$ $$\varepsilon_1 = \varepsilon_x + \varepsilon_z + \varepsilon_2 \quad (10)$$ $$\gamma_{xz} = 2(\varepsilon_x + \varepsilon_2)\cot\theta \quad (11)$$ Crack widths: $$w = \varepsilon_1 s_\theta \quad (12)$$ $$s_\theta = 1/\left(\frac{\sin\theta}{s_x} + \frac{\cos\theta}{s_z}\right) \quad (13)$$	$$f_{sx} = E_s\varepsilon_x \le f_{yx} \quad (14)$$ $$f_{sz} = E_s\varepsilon_z \le f_{yz} \quad (15)$$ Concrete: $$f_2 = \frac{f_c'}{0.8 + 170\varepsilon_1}\left[\frac{2\varepsilon_2}{\varepsilon_0} - \left(\frac{\varepsilon_2}{\varepsilon_0}\right)^2\right] \,(16)$$ $$f_1 = \frac{0.33\sqrt{f_c'}}{1 + \sqrt{500\varepsilon_1}} + \sigma_f \quad (17)$$ Shear stress on crack: $$v_{ci} \le \frac{0.18\sqrt{f_c'}}{0.31 + \dfrac{24w}{d_a + 16}} + v_f \quad (18)$$

Where ρ_x and ρ_z = the reinforcement ratios in the longitudinal and transverse direction; f_c'= cylinder compressive strength; d_a = maximum aggregate size; f_{sx}, f_{sz} = average stresses in the longitudinal and transverse reinforcement; f_1= average tensile stress; f_2= average compressive stress; θ= inclination of the diagonal compressive; v= shear strength; ε_x= average longitudinal strain; ε_y= average transverse strain; ε_2= principal compressive strain; ε_1= principal tensile strain; v_{ci} = shear stress on the crack face; w = average crack width; S_θ= average crack spacing; S_x, S_z = indicators of the crack control characteristics of the x-reinforcement and the z-reinforcement.

The relationships mentioned in Table 1 of the proposed theory can be used to predict the shear strength of a SFRSCC beam. Assuming that the shear stress in the web is equal to the shear force divided by the effective shear area $b_w d_v$, and that, at failure, the stirrups will yield, equilibrium Eqn. (5) can be rearranged to give the following expression for the shear strength V_n of the section

$$V_n = V_c + V_s \tag{19}$$

$$V_n = f_1\, b_w\, d_v\, \cot\theta + A_v f_y d_v \cot\theta/s \tag{20}$$

In this case for design, the fibre distribution is assumed to be three dimensional (spatial portions) [24-25].

$$\sigma_f = \alpha\tau_f V_f (1+f)/3 \tag{21)/ [23]}$$

Therefore, if we consider the fibre effect on the shear capacity, we can get Eqn. (22) and Eqn. (23) as follows:

$$V_n = [v_{ci} + \alpha\tau_f V_f(1+f)(1+\cot\theta)/3]b_w d_v + A_v f_y d_v \cot\theta/s \tag{22}$$

$$V_n = [\beta\sqrt{f_c'} + \alpha\tau_f V_f(1+f)(1+\cot\theta)/3]b_w d_v + A_v f_y d_v \cot\theta/s \qquad (23)$$

The proposed Eqn. (23) is a modified version of the 2004 CSA expression for calculating of the ultimate shear capacity of SFRC beams. The determination of β and θ is based on the 2004 CSA general method [26-27].

3 EXPERIMENTAL PROGRAM

3.1 Materials

In this test program, the concrete mixture was made with ordinary Portland cement (CEM I 42.5), fly ash, natural sand (0–5 mm), crushed gravel of 10 mm maximum size. To improve the workability, a ploycarboxylic acid-based high-range water-reducing admixture (HRWRA), was added after extensive trials. Table 2 summarizes the mixture proportions of SFRSCC employed in this testing program. The hooked-ended macro steel fibre RC-80/60-BN (fibre length $l_f = 60$ mm, equivalent diameter $d_f = 0.75$ mm, aspect ratio $l_f/d_f = 80$, ca. 15,000 pieces/kg, tensile strength 1100 N/mm^2) was used (Fig. 2). The fibre contents added into the mixture were 0, 20 kg/m^3, 40 kg/m^3 and 60 kg/m^3. The details of the deformed steel bars with a diameter of 16 mm as longitudinal reinforcement can be seen in the Fig. 3. Hot-rolled plain bars with a diameter of 6.5 mm (Φ6.5) and a diameter of 8 mm (Φ8) were used as stirrups and the top longitudinal reinforcement respectively. The longitudinal reinforcement and stirrup had a yield stress of 430 MPa and 300 MPa with an ultimate stress of 650 MPa and 500 MPa respectively.

Table 2 Mix propottion

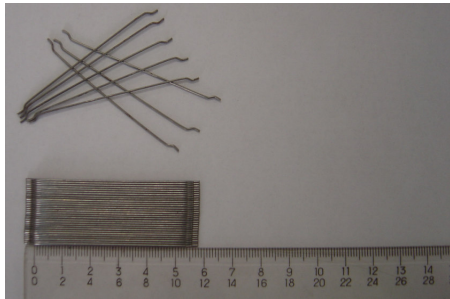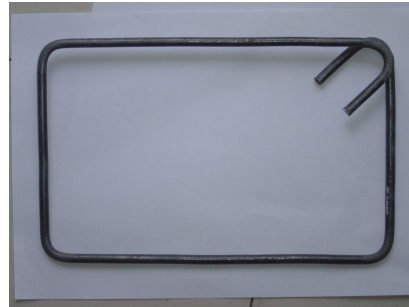| Cement /kg·m^{-3}	Fly ash /kg·m^{-3}	Water /kg·m^{-3}	Sand /kg·m^{-3}	Gravel /kg·m^{-3}	Super-plasticizer (%)	W/B
400	170	200	742	724	1.40	0.35

Fig. 2 Macro steel fibres


Fig. 3Stirrup

3.2 Test specimens

A series of steel fibre reinforced SCC beams were tested. All beams with a dimension of B (width) x H (depth) x L (length) = 100 mm x 150 mm x 1400 mm, were tested on a span of l_s = 1140 mm. The beams had three different stirrup ratios (ρ_v) and three different fibre contents. The longitudinal reinforcement ratio (ρ_s = 3.35%) and the shear span-to-depth ratio (a/d = 4), were kept constant. More details of the test specimens are illustrated in Table 3. Longitudinal tensile reinforcement has 90-degree hooks at the beam ends to ensure adequate anchorage, and additional stirrups were provided at the concentrated loading point of midspan and support for preventing of the local failure. The specimen dimension and reinforcement layout are shown in Fig. 4.

Table 3 Details of test beams

Beam No.	Dimension /mm	a/d	Stirrup ratio / %	Stirrup spacing /mm	Fibre content /kg·m^{-3}
SSF0-∞		4	0	∞	0
SF20-∞		4	0	∞	20
SF40-∞		4	0	∞	40
SF60-∞		4	0	∞	60
SF0-480		4	0.138	480	0
SF20-480		4	0.138	480	20
SF40-480	b=100	4	0.138	480	40
SF60-480	h=150	4	0.138	480	60
SF0-240	l_s=1140	4	0.275	240	0
SF20-240		4	0.275	240	20
SF40-240		4	0.275	240	40
SF60-240		4	0.275	240	60
SF0-160		4	0.413	160	0
SF20-160		4	0.413	160	20
SF40-160		4	0.413	160	40
SF60-160		4	0.413	160	60
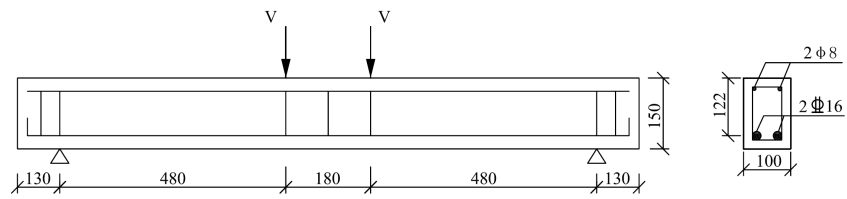
(a) Reinforcement detail of SF-∞
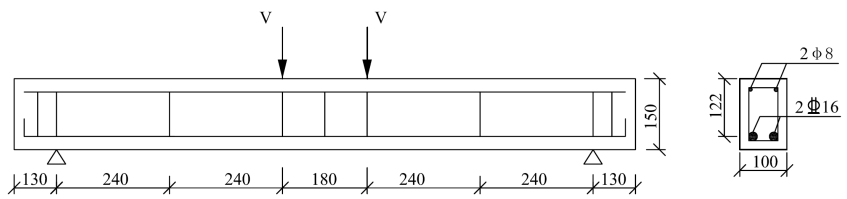
(b) Reinforcement detail of SF-480
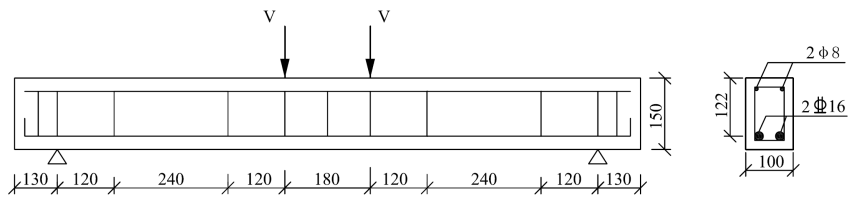
(c) Reinforcement detail of SF-240

(d) Reinforcement detail of SF-160

Fig. 4 Dimension and reinforcement details of test beams (units: mm)

Fig. 5 Loading and measuring arrangement of test beams (units: mm)

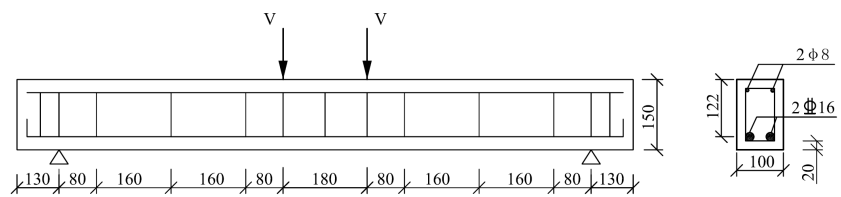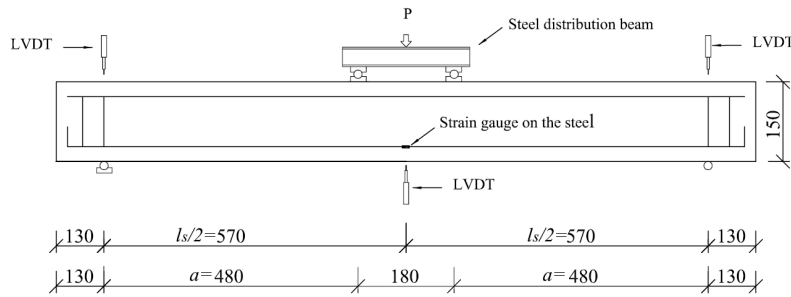## 3.3 Testing procedures

3.3.1 Properties of fresh and hardened concrete

The workability of fresh SCC was evaluated according to the reference [28-29]. The test methods used in this research included slump flow test (for assessing the workability and filling ability), L-box test (for assessing passing ability and flowability). They were sufficient to monitor production quality. In order to simulate the reinforcement ratio of the beam, the steel ratio of the L-box was equal to that of RC beam ($\rho_s = 3.35\%$).

The 28-day concrete compressive strength was measured using 150x150x150 mm cubic specimen following the Chinese guideline [30].

3.3.2 Experimental beam test setup

Monotonic loading was provided with a 10000 kN hydraulic servo testing machine using a steel distribution beam with special bearing assemblies on the top face of the beam. The tests for load - displacement responses were deformation-controlled and the deformation rate of test was 0.2 mm/min [31]. The vertical deflection at the mid-span was monitored and recorded by a linear voltage differential transformer (LVDT) installed around the test beam. Electrical-resistance strain gages were used to record the strains in the concrete as well as reinforcement at several selected locations, as shown in Fig.5.

4 EXPERIMENTAL RESULTS

4.1 Workability and compressive strength

The experimental results of workability of steel fibre reinforced fresh SCC are presented in Table 4. The factor d_m represents the average final diameter, while factor T_{500} represents the time taken for the mixture to reach the 500 mm spread circle in slump flow test. Parameters T_{200} and T_{400} represent the time taken for the mixture to reach 200 mm and 400 mm in the L-box. The ratio H_2/H_1 represents the blocking in the in the L-box. It can be seen from Table 4 that all parameters regarding workability meet the requirements of SCC according to

EFNARC [28]. When steel fibre content is 60 kg/m^3, the value of H_2/H_1 is low which just fulfilled the requirements. It means that the steel fibre content of 60 kg/m^3 could achieve the upper limit of the workability of SFRSCC, when the steel ratio (ρ_s) of RC beam arrives 3.35%. The typical slump flow test and L-box test for SFRSCC mixture is depicted in Fig. 6.

The cubic compressive strength f_{cu} and equivalent cylinder compressive strength f'_c of steel fibre reinforced SCC at 28 days are also listed in Table 4. The addition of fibres aids in converting the brittle properties of concrete into a ductile material, however no significant trend of improving compressive strength was observed.

Table 4 Fresh and mechanical properties of SFRSCC mixture

Fibre contents /kg·m^{-3}	Slump flow			L-box		$f_{cu,28}$ / MPa	$f'_{c,28}$ / MPa
	d_m /mm	T_{500} /s	H_2/H_1	T_{200} /s	T_{400} /s		
0	780	4.2	0.89	2.2	5.1	39.3	33.8
20	760	4.0	0.85	2.8	5.5	41.9	36.0
40	740	3.8	0.83	3.0	5.8	37.8	32.5
60	700	3.7	0.78	5.0	10.0	47.9	41.2

(a) Slump flow test   (b) L-box test

Fig. 6 Tests of workability of SCC with 60 kg/m^3 fibres
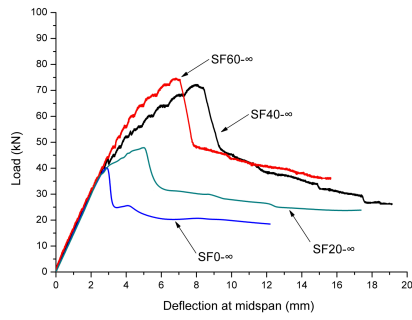
4.2 Load-deflection behaviour

Fig. 7 presents the effect of fibre addition on the load-midspan deflection for the SFRSCC

beams. The addition of steel fibres may enhance the cracking load and ultimate load of SCC beams.

Shear failure occurred in all beams without stirrups (Fig. 7a). The beam SF0-∞ showed both lower ultimate load carrying capacity (F_u = 40.7 kN) and brittle failure pattern. After the ultimate load F_u, the beam SF0-∞ showed low post-peak behaviour and the load carrying capacity declined abruptly. Compared to the beam SF0-∞, F_u of a beam with 20 kg/m^3 steel fibres (SF20-∞) increased about 17.8%. It can be observed that the beam without fibres failed soon after the first diagonal crack appeared. However, the addition of steel fibres can change the brittle failure pattern of a beam into a more ductile one. More closely spaced cracks were observed in fibre reinforced beams than those without fibres. The crack spacing and crack width under the same load clearly declined with the increasing of fibre content (Fig. 8). The steel fibres became effective after cracking, with a more evenly stress redistribution over the cracking region, and continued to resist the tensile stresses until the pullout of the fibres.

In comparison with beam SF0-480, the addition of 20 kg/m^3 and 40 kg/m^3 steel fibres can enhance the ultimate load F_u by about 33% and 61.5% respectively. However, the beams with only 20 kg/m^3 and 40 kg/m^3 steel fibre still exhibited some brittle diagonal failure patterns. After F_u, the load carrying capacity decreased clearly (Fig. 7b). The addition of 60 kg/m^3 steel fibres can transform the brittle shear failure pattern of SF0-480 into a well ductile flexure failure pattern of SF60-480. This means that the addition of 60 kg/m^3 steel fibres had a strong effect on the failure pattern and deformability of conventional steel rebar reinforced beam. It also indicated high composite effect efficiency between steel fibres and stirrups. The beams with a stirrup spacing of 240 mm and 160 mm (Fig. 7 (c) and (d)) followed the same trend.

Generally, for each stirrup ratio (ρ_v = 0 in Fig.7(a), 0.138% in Fig.7(b), 0.275% in Fig.7(c) and 0.413% in Fig.7(d)), following three points can be observed:
- The post-peak behaviour and the ductility of concrete beams increased clear with the increasing of fibre dosage.
- The failure pattern of SCC beams is transformed gradually from the brittle shear failure into a ductile flexure failure with the increasing of fibre dosage.
- The well distributed fibres in beam acting as a three dimensional net [4-6] can also transfer the tensile force, hence, the post crack behaviour of steel fibre reinforced RC beams show a great improvement compared to those of SCC without fibres or only with stirrups.

(a) SF-∞
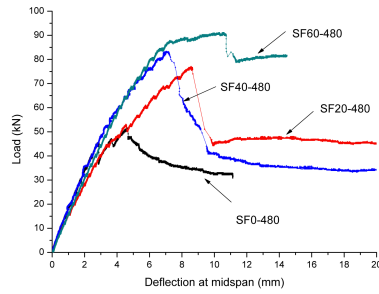
(b) SF-480
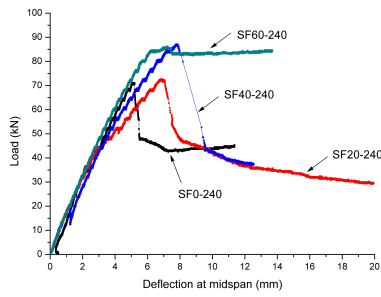
(c) SF-240
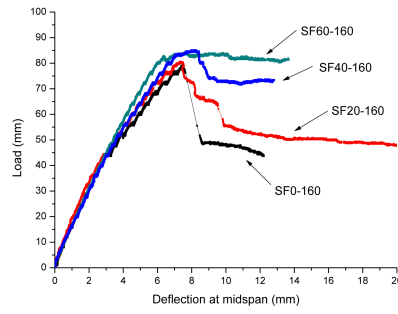
(d) SF-160

Fig. 7 Load-deflection responses with different stirrup ratios

(a) SF0-∞
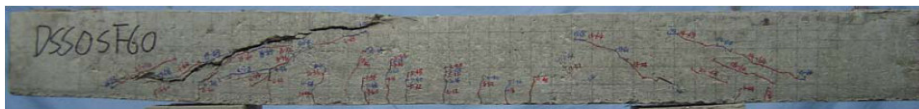
(b) SF60-∞

Fig. 8 Cracks and failure patterns of beams witout stirrups

4.3 Toughness

In this study, the post-peak behaviour of test beams in terms of flexural toughness parameters was evaluated. According to the reference [5], two toughness parameters (D^f_8, $f^f_{eq.8}$) were introduced to evaluate the energy absorption capacity and the residual load bearing capacity of the test beams to a deflection $\delta_8 = \delta_{cr} + 8$ mm. D_8 can be defined as the area under load-deflection curve, which is the total energy absorbed up to the certain deflection δ_8 of the beam. The equivalent strength $f^f_{eq.8}$ can be determined by means of the following expressions:

$$f^f_{eq.8} = D^f_8 l_s / 6 b_w d_v^2 \tag{24}$$

The calculated results of energy absorption and equivalent strengths of test beams with different stirrup ratios are presented in Table 5. It can be seen that the beam only with stirrups (SF0-480, SF0-240) showed relatively low toughness. The combined using of stirrups and steel fibres demonstrated a positive hybrid effect in improving the post-peak behaviour as well as toughness of test beams (see Fig. 7 and Fig. 9).

Fig. 9 presents the hybrid effect of stirrups ($\rho_v = 0.138\%$, 0.275%) and steel fibres on toughness parameter ($f^f_{eq.8}$). It can be seen that a steel fibre content of 20 kg/m^3 can replace at least a stirrup ratio of 0.137%. It means that the addition of 20 kg/m^3 steel fibres can enlarge the stirrup spacing from 240 mm to 480 mm. The combined use of stirrups and steel fibres demonstrates strong positive hybrid effect on shear load-carrying capacity, the post-crack behaviour and toughness of SCC beams subjected to shear and bending.

Table 5 Comparison of energy absorption and equivalent flexural strength

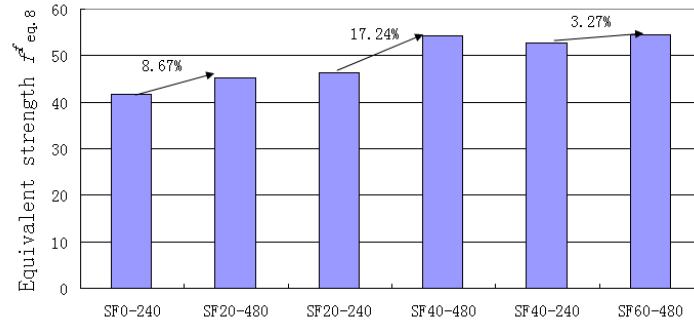| Beam No.	D^f_8 /(kN.mm)	$f^f_{eq.8}$ /(N/mm^2)
SF0-∞	190.35	24.30
SF20-∞	287.81	36.74
SF40-∞	367.74	46.94
SF60-∞	385.02	49.15
SF0-480	284.42	36.31
SF20-480	354.08	45.20
SF40-480	425.65	54.34
SF60-480	426.49	54.44
SF0-240	325.83	41.59
SF20-240	363.06	46.35
SF40-240	412.98	52.72
SF60-240	440.69	56.26
SF0-160	386	49.27
SF20-160	406.69	51.92
SF40-160	425.95	54.25
SF60-160	438.6	55.99

Fig. 9 Increase ratio of the toughness parameter for beams with different reinforcements

The positive hybrid effect of stirrups and steel fibres on the concrete member can demonstrate some advantages as follows:
● Enhancing of the residual load-bearing capacity in the post-peak zone greatly
● Changing the failure pattern from a brittle diagonal shear failure into a ductile bending failure pattern with the increasing of fibre dosage
● Replacing of the stirrups of RC members, only 20 kg/m^3 steel fibres can replace partially stirrups and enlarge the stirrup spacing from 240 to 480 mm.

   Besides, the combined application of stirrups and steel fibres in concrete beam can also 1) reduce the construction period and the cost of assembling reinforcement, 2)affect the concrete casting and 3) improve the concrete quality and 4) increase the bond behaviour between the steel rebar and concrete matrix.

   Steel fibres, which are well distributed three-dimensionally in the beam, can orientate parallel to the trajectory of the principle tensile stress, they are efficient to resist the diagonal shear force and work partly as shear reinforcement. Therefore, the joint action of fibres and stirrups are more effective in arresting diagonal crack propagation than that of mono reinforcement and can greatly increase the shear capacity and ductility.

4.4 Shear cracking load and ultimate load

   The shear cracking load F_{cr} (diagonal cracking load) , the ultimate load F_u and the failure mode are summarized in Table 6. A careful examination of these results indicates that both F_{cr} and F_u (= $2V_{u,exp}$) of SFRSCC beams are influenced by the fibre content and the stirrup ratio. Table 6 shows that the effect of fibre content on F_{cr} and F_u of the test beams with different stirrup ratios. Form Table 6 it can be seen that the shear cracking load F_{cr} increases with the increasing of the fibre content and the increase rate is low as ρ_v becomes bigger. The maximum increase rate in F_{cr} was about 200% for beam SF60-∞. The maximum increase in F_u was about 82.3% for the beam SF60-∞. With the increase of stirrup ratio, the beams failed in flexure and the applied load at failure was determined by the yield of longitudinal reinforcement or crush of concrete. Therefore, the ultimate load did not increase clearly with

the increasing of fibre content at high stirrup ratios.

Table 6 Comparisons between predicted and observed loads

Beam no.	F_{cr}/ kN	F_u/ kN	$V_{u, exp}$ / kN	$V_{u, pre}$ / kN	failure Pattern	$V_{u, exp}$ / $V_{u, pre}$
SF0-∞	10	40.7	20.35	-	shear	-
SF20-∞	15	48.00	24.00	19.07	shear	1.259
SF40-∞	19.6	72.22	36.11	26.51	shear	1.362
SF60-∞	30.2	74.65	37.33	36.32	shear	1.028
SF0-480	10.6	51.53	25.77	-	shear	-
SF20-480	16.1	77.07	38.54	26.09	shear	1.477
SF40-480	20.5	83.23	41.62	33.53	shear	1.241
SF60-480	20.8	91.16	45.58	43.34	flexure	1.052
SF0-240	12.1	68.04	34.02	-	shear	-
SF20-240	14.2	72.66	36.33	33.10	shear	1.098
SF40-240	15.2	86.98	43.49	40.55	shear	1.072
SF60-240	16.1	86.32	43.16	50.36	flexure	0.857
SF0-160	15	79.27	39.64	-	shear	-
SF20-160	17	80.59	40.30	40.12	shear	1.005
SF40-160	21	84.56	42.28	47.56	flexure	0.889
SF60-160	21.3	84.12	42.06	57.37	flexure	0.733
						Mean = 1.089
						CV = 0.198

4.5 Prediction and comparison

In addition to the tensile capacity of the fibres, the traditional CSA expression is modified to account for the improvement in dowel action imparted by the fibres and the enhancement of the interlocking of aggregates. Based on the regression analysis, the Eqn. (23) is modified to the following proposed equations:

For SFRSCC beams:

$$V_n = [\beta\sqrt{f_c'} + \alpha\tau_f V_f(1+f)(1+\cot\theta)/3]b_w d_v + A_v f_y d_v \cot\theta/s \qquad (25\ a)$$

For SFRC beams:

$$V_n = 4d/a[\beta\sqrt{f_c'} + \alpha\tau_f V_f(1+f)(1+\cot\theta)/3]b_w d_v + A_v f_y d_v \cot\theta/s \qquad (25\ b)$$

The ultimate load prediction of test beams was made using the proposed methods for shear and compared with the corresponding measured failure load ($V_{u,exp}$) in Table 6.

To extend the validity of the proposed method for the shear strength, the prediction was made for beams that had been tested in previous studies. For FRSCC, the investigation was limited to slender beams ($a/d \geq 3$) due to the lack of experimental data. The dimensions and properties are summarized in Table 7. A comparison of the experimental-to-predicted shear capacity data for the modified CSA expression is also presented in Fig. 10 along with the associated coefficient of determination (R^2), mean absolute error (MAE), and the average measured -to-predicted shear capacity ratio (V_m/V_p).
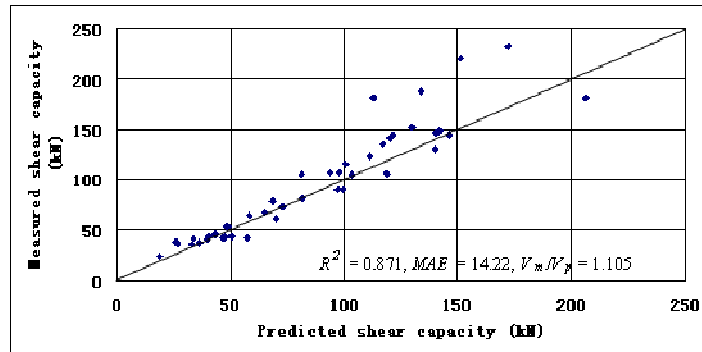
Fig. 10 Measured shear capacity versus predicted values by modified CSA equation

By comparing measured and predicted ultimate loads in Table 7 and Fig. 10, it can be seen that the solutions based on the proposed method correlate well with the experimental results of fibre reinforced SCC beams without stirrups, having a mean of 1.07 and a CV (coefficient of variation) of 0.095. However, the proposed method provides a conservative prediction for

the shear capacity of fibre reinforced SCC beams with stirrups, having a mean of 1.380 and a CV of 0.098. This may be attributed to the influence of the longitudinal reinforcing steel and stirrups on the shear capacity of fibre reinforced RC beams, which becoming more pronounced with the addition of fibres. Despite its better fit, the modified CSA equation is not conservative for any of the three data sets (Ashour et al, Kwak, Tom Greenough), but with the incorporation of a reduction factor it could provide a reliable and conservative prediction of the shear capacity for beams without stirrups.

Table 7 Summary of beam details and comparison of experimental and predicted shear strengths

Investigator	Beam no.	Fibre type	V_f(%)	l_f/d_f	f_c'	b_w	d_v	a/d	ρ_s(%)	f_{ys}	d_a	ρ_v(%)	f_{yv}	s	$V_{u,exp}$	$V_{u,predicted}$	$V_{u,exp}/V_{u,predicted}$
Ashour et al [9]	B-2-0.5-A	Hooked	0.5	75	99.1	125	215	2.0	2.84	460	10				129.54	140.2	0.924
	B-4-0.5-A		0.5	75	95.4	125	215	4.0	2.84	460	10				61.01	70.1	0.870
	B-6-0.5-A		0.5	75	95.83	125	215	6.0	2.84	460	10				42.73	46.73	0.915
	B-2-1.0-M		1.0	75	94.5	125	215	2.0	4.58	470	10				180.87	206.24	0.873
	B-4-1.0-M		1.0	75	93.8	125	215	4.0	4.58	470	10				104.28	103.12	1.011
	B-6-1.0-M		1.0	75	95.0	125	215	6.0	4.58	470	10				78.74	68.75	1.146
																Average=0.957 CV=0.111	
Kwak [12]	FHB2-2	Hooked	0.5	62.5	63.8	125	212	2.0	1.5	442	19				134.89	117.09	1.152
	FHB3-2		0.75	62.5	68.6	125	212	2.0	1.5	442	19				144.16	146.21	0.986
	FHB2-3		0.5	62.5	63.8	125	212	3.0	1.5	442	19				81.89	81.56	1.004
	FHB3-3		0.75	62.5	68.6	125	212	3.0	1.5	442	19				90.1	97.41	0.925
	FHB2-4		0.5	62.5	63.8	125	212	4.0	1.5	442	19				63.87	58.54	1.091
	FNB3-4		0.75	62.5	68.6	125	212	4.0	1.5	442	19				72.61	73.12	0.993
	FNB2-2		0.5	62.5	30.8	125	212	2.0	1.5	442	19				107.06	97.68	1.096
	FNB2-3		0.5	62.5	30.8	125	212	3.0	1.5	442	19				67.58	65.17	1.037
	FNB2-4		0.5	62.5	30.8	125	212	4.0	1.5	442	19				53	48.85	1.085
																Average=1.041 CV=0.075	
Greenough, T. [16]	S-HE-50-0.5	Hooked	0.5	50	43.9	200	265	3	1.7	400	10				90.85	99.74	0.911
	S-HE-50-0.75	Hooked	0.75	50	39.7	200	265	3	1.7	400	10				105.6	118.77	0.889
	S-HE-50-1.0	Hooked	1.0	50	41.7	200	265	3	1.7	400	10				148.9	141.87	1.050
	S-FE-50-0.5	Hooked	0.5	50	45.3	200	265	3	1.7	400	10				115.5	100.63	1.148
	S-FE-50-0.75	Flat end	0.75	50	44.0	200	265	3	1.7	400	10				144.1	121.59	1.185
	S-FE-50-1.0	Flat end	1.0	50	39.9	200	265	3	1.7	400	10				146.8	140.68	1.044
	S-FE-30-0.5	Flat end	0.5	43	44.4	200	265	3	1.7	400	10				106.7	93.96	1.136
	S-FE-30-0.75	Flat end	0.75	43	42.4	200	265	3	1.7	400	10				122.9	111.41	1.103
	S-FE-30-1.0	Flat end	1.0	43	41.7	200	265	3	1.7	400	10				151.4	129.68	1.167
																Average=1.070 CV=0.095	
Ding Y [17]	SFSCCB25-∞	Hooked	0.32	65	36	200	262	3	2.6	460	10				105.26	81.38	1.293
	SFSCCB50-∞		0.64	65	41.7	200	262	3	2.6	460	10				140.59	120.06	1.171
	SFSCCB25-250		0.32	65	36	200	262	3	2.6	460	10	0.132	340	250	180.91	112.72	1.605
	SFSCCB50-250		0.64	65	41.7	200	262	3	2.6	460	10	0.132	340	250	220.87	151.4	1.459
	SFSCCB25-150		0.32	65	36	200	262	3	2.6	460	10	0.22	340	150	187.63	133.61	1.404
	SFSCCB50-150		0.64	65	41.7	200	262	3	2.6	460	10	0.22	340	150	232.91	172.3	1.352
																Average=1.380 CV=0.098	

5 CONCLUSIONS

The following conclusions can be drawn from the experimental program on a series of steel fibre reinforced SCC beams with various parameters.

1. The equations to predict shear capacity, based on the concept of modified compression field theory, are proposed in which cracked fibre concrete is treated as a new material with its own stress-strain characteristics. A new equation of modified compression field theory for fibre reinforced concrete is proposed.

2. The addition of 60 kg/m^3 steel fibres was the upper bound of the fibre content regarding the workability of SCC members with a reinforcement ratio 3.35%.

3. Steel fibres can enhance the shear cracking load and ultimate load of SCC beams. For fibre addition of 60 kg/m^3, the maximum shear capacity of SCC beams without stirrups was increased by up to 82% over that of beam without fibres.

4. The diagonal shear as the cause for brittle failure in fibre reinforced SCC beams with different stirrup ratios ($\rho_v \leq 0.413$) changes to a mainly ductile flexural failure of fibre reinforced SCC beams when the fibre content achieves 60kg/m^3.
5. The addition of 20 kg/m^3 fibres can partly replace the conventional stirrups and enlarge the stirrup spacing from 240 mm to 480 mm, namely reducing the stirrup ratio about 0.137% in this study.
6. The combined use of stirrups and steel fibres shows great positive composite effect on shear load-carrying capacity, energy absorption capacity and toughness of SCC beams subjected to shear and bending.
7. The modified CSA equation for design to predict shear capacity was proposed. The accuracy of the proposed equation is validated using experimental data obtained on SFRC beams by the authors and other researchers. It is found to be simple and capable to provide reasonable estimates for the shear capacity of SFRC beams, and is thus suitable for implementation in design provisions after further validation.

NOTATION

α	The aspect ratio
l_f	Fibre length
d_f	Equivalent diameter
ρ_s	The longitudinal reinforcement ratio
ρ_v	Stirrup ratios
a/d	Shear span-to-depth ratio
$f_c{}'$	Cylinder compressive strength
d_a	Maximum aggregate size
f_f	Load of a single fibre transferred intersects at crack
σ_f	Load component of a single fibre transferred perpendicular to crack
v_f	Load component of a single fibre transferred parallel to crack
SFRSCC	Steel fibre-reinforced self-consolidating concrete
SF40-240	Steel fibre-reinforced self-consolidating concrete beams with 40 kg/m^3 steel fibre content and a 240 mm spacing of stirrup
b_w	Width of the beam cross section
d_v	Effective depth of the beam cross section

h	Depth of the beam cross section
d_m	The average of final diameter in slump flow test
f_{yl}	Yield stress of longitudinal reinforcement
f_{yst}	Yield stress of stirrup
T_{500}	The time for concrete to reach the 500mm spread circle in the slump test
T_{200}, T_{400}	Time taken for the mixture to reach 200 mm and 400 mm in the L-box test
H_2/H_1	The blocking ration in the L-box test
F_{cr}	Shear cracking load
F_u	The ultimate load

REFERENCE

1. ACI Committee 544. State-of-the-art report on fiber reinforced concrete (ACI 544.IR-96). American Concrete Institute, Farmington Hills, Mich., 1997. p. 1-60.
2. Corinaldesi V, Moriconi G. Durable fiber reinforced self-compacting concrete. Cement and Concrete Research 2004; 34(2):249–254.
3. Sorelli L, Toutlemonde F. On the design of steel fibre reinforced concrete tunnel lining segments. In: 11th International conference on fracture; 2005.
4. Ding Y, You ZG, Jalali S. Hybrid fibre influence on strength and toughness of RC beams.Composite Structures 2010; 92(9): 2083-2089 .
5. Ding Y, et al. Experimental investigation on the mechanical of the fibre reinforced high-performance concrete tunnel segment. Composite Structures 2011; 93(4):1284-1289.
6. Ding Y, Kusterle W. Comparative study of steel fibre-reinforced concrete and steel mesh-reinforced concrete at early ages in panel tests. Cement and Concrete Research 1999; 29(11): 1827–1834.
7. Sharma AK. Shear strength of steel fiber reinforced concrete beams. ACI Journal 1983; 83(4):624-628.
8. Narayanan R, Darwish IYS. Use of steel fibres as shear reinforcement. ACI Structural Journal1987; 84(3): 216-227.
9. Ashour SA, Hasanain GS, Wafa FF. Shear Behaviour of high-strength fiber-reinforced concrete beams. ACI Structural Journal 1992; 89(2):176-184.
10. Adebar P, et al. Shear tests of fibre concrete beams without stirrups. ACI Structural Journal 1997; 94(1):68–76.
11. Lim DH, Oh BH. Experimental and theoretical investigation on the shear of steel fibre reinforced concrete beams. Engineering Structures 1999; 21(10):937-944.
12. Kwak Y, et al. Shear strength of steel fiber-reinforced concrete beams without stirrups. ACI Structural Journal 2002, 99(4): 530-538.
13. Cho S, Kim Y. Effects of steel fibers on short beams loaded in shear. ACI Structural Journal 2003; 100(6): 765–774.
14. Cucchiara C, La Mendola L, Papia M. Effectiveness of stirrups and steel fibres as shear reinforcement. Cement and Concrete Composites 2004; 26 (7): 777-786.

15. Meda A, Minelli F, Plizzari G P, Riva P. Shear behaviour of steel fibre reinforced concrete beams. Materials and Structures 2005; 38(4):343-351.
16. Greenough T, Nehdi M. Shear behaviour of fiber-reinforced self-consolidating concrete slender beams. ACI Materials Journal 2008; 105(5): 468-477.
17. Ding Y, You Z, Jalali S. The composite effect of steel fibres and stirrups on the shear of beams using self-consolidating concrete. Engineering Structures 2011; 33(1):1107-117.
18. Minelli F, Vecchio J. Compression field modeling of fiber reinforced concrete members under shear loading. ACI Structural Journal 2006; 103(2): 244-252.
19. Joint ACI-ASCE Committee 445. Recent approaches to shear design of structural concrete. Journal of Structural Engineering, ASCE 1998; 124(12): 1375-1417.
20. Vecchio FJ, Collins MP. The modified compression field theory for reinforced concrete elements subjected to shear. ACI JOURNAL 1986; 83(2):219-231.
21. Collins MP, Mitchell D, Adebar P, Vecchio FJ. A general shear design method. ACI Structural Journal 1996; 93(1): 36-45.
22. Bentz EC, Vecchio FJ, Collins MP. Simplified modified compression field theory for calculating shear strength of reinforced concrete elements. ACI Structural Journal 2006; 103(4): 614-624.
23. Collins MP, Mitchell D. Prestressed Concrete Structures. Englewood Cliffs: Prentice Hall, 1991.
24. Stroeven P, Hu J. Effectiveness near boundaries of fibre reinforcement in concrete. Materials and Structures 2006; 39: 1001-1013.
25. Stroeven P. Stereological principles of spatial modeling applied to steel fibre-reinforced concrete in tension. ACI Material Journal 2009; 106(3) 213-222.
26. CSA Committee A23.3. Design of Concrete Structures (CSA A23.3-04). Canadian Standards Association, Mississauga, 2004.
27. Bentz EC, Collins MP. Development of the 2004 CSA A23.3 Shear Provisions for Reinforced Concrete. Canadian Journal of Civil Engineering 2006; 33(5): 521-534.
28. EFNARC. Specification and guidelines for self-compacting concrete; 2002.
29. The SCC European Project Group. The European Guidelines for Self-Compacting Concrete Specification. Production and use; 2005.
30. China standardization association of engineering construction standard CECS 13-2009. Testing methods of steel fibre reinforced concrete; 2009.
31. National Standard of the People's Republic of China. Test methods of concrete structures (GB50152-92). Beijing: China Architecture & Building Press, 1992 [in Chinese].